Supplementary materials:

This PDF file includes:
Materials and Methods
Figures and legends S1 to S11

Materials and Methods

Transgenic lines

Genomic sites of insertions were determined by inverse PCR (BDGP methods); in situ hybridization of salivary glands polytene chromosomes with a CaSpeR-AUG-β-gal vector as a probe was done to confirm the presence of single transgene in the line. Transformant lines which were analyzed for each piRNA pathway gene mutations are listed below (cytological position of transgene is indicated in brackets):

piwi: H12 (9D), H18 (66C), H111 (96D);
spn-E: H12 (9D), H95 (55C), H124 (53F);
aub: H18 (66C), H111 (96D).

5' RACE analysis

RNA was extracted from dissected ovaries of the *z2* line (Fig. 1) or H18 transgenic line using TRIzol reagent (Invitrogen). RNA samples were treated with TURBO DNase (Ambion). 5'RACE analysis was performed using the 5' RACE system (Invitrogen) according to the manufacturer's general guidelines. *yellow*-specific primers for the first strand cDNA synthesis and PCR were 5'-AATATAATCTCCACTAGCCAG-3' and 5'-AAGACGGCGTCACCAAGGTGATC-3', respectively. Primers for the first strand cDNA synthesis and PCR, corresponding to the CaSpeR-AUG-β-gal sequence, were 5'-GAAAATCACGTTCTTGTTG-3' and 5'-TGGTCAAAGTAAACGACATGGTGAC-3', respectively.

RTqPCR analysis

cDNA was synthesized using random hexamers and SuperScriptII reverse transcriptase (Invitrogen). DNA samples were analyzed by real-time quantitative PCR using SYTO-13 incorporation (Invitrogen). For qPCR we used DT-96 machine from DNA Technology, Russia. The primers which were used are represented below. Eight serial 3-fold dilutions of genomic DNA of corresponding line were amplified in duplicates with each primer pair to make a standard curves. Standard curves were used for extrapolation of expression level for the samples to be tested based on their threshold cycle values. The determined values were averaged and normalized with the concentration of ribosomal protein gene *rp49* transcripts. All experiments were performed with at least two independent RNA samples; each sample was analyzed in duplicate.

Primers for RT-PCR and ChIP analysis

rp49 5'-ATGACCATCCGCCCAGCATAC-3' and 5'-GCTTAGCATATCGATCCGACTGG -3'

HeTA/yellow (H1) 5’- CTGTCTCCGTACCTCCACCAGC-3’ and (y) 5’-CTCCTGAAGTTTGTAAGCAGCCCA-3’
HeTA/lacZ (H1) 5’- CTGTCTCCGTACCTCCACCAGC-3’ and 5’-TAAGAATTCTGCTTTAGCAGGCTCTTTCGATC-3
H2 5’-ATATTACAAAAATTGTAATCAAAGGCAA-3’
β-gal 5’-TTCCAGTTCAACATCAGCCGCTAC-3’ and 5’-GTTGATGTCATGTAGCCAAATCGG-3’
piwi 5‘-CCGAGCATCGAGAATCCT’-3 and 5’-AAGTCCAAAACATTTACCCG’-3’
HeT-A 5’-GGAGTGATGAGCGGCGGAAA-3’ and 5’-CCAGGCAAGCGGACAAACGA-3’
TART-A1 5’-AATGAACTTTGTCTGCCCTCCCA-3’and 5’-ATCTGTCTACTGTCCGCCTTCGCTA-3’
HMS Beagle 5’- CGGCTGCGTGAACCAAAGTG-3’ and 5’-CGGGCTGCTGCTGCTGCTAC-3’
I-element 5’-ACAAAATCACTTCAAAAACATACCAATCCC-3’ and 5’-GCATCCCTCAACTTCTCCTCCACAG-3’
1731 5’-ATGTTTGTGGAAGGTGGTTTCAGG-3’ and 5’-GCTTTTTCATCTTGGGATTGCC-3’
copia 5’-CGACAGTGTGGAGGTTGTGCC-3’ and 5’-CTTGGAGACGCTTTACGGACAT-3’
60D intergenic spacer 5’-CGGCGAGGGGGGAAAAGGAC-3’ and 5’-CTTGGCAGCAGGTGGAAAATGTT-3’

Quantitative β-galactosidase activity assay

To measure β-galactosidase activity, ten pairs of hand-dissected ovaries were added to 200 μl of Z buffer (60 mM Na_2HPO_4, 40 mM NaH_2PO_4, 10 mM KCl, 1 mM $MgSO_4$, 0.35% β-mercaptoethanol) and were homogenized, then 100 μl of 0.4% ONPG (*o*-nitrophenyl-β-D-galactopyranoside) in Z buffer was added. Samples were incubated at 37°C for 2 h, and the reaction was stopped by adding of 1 ml 0.52 M Na_2CO_3. The extracts were centrifuged at 20,000 g for 1 min. β-galactosidase activity was calculated from absorbance measured at 420 and 550 nm. The experiment was repeated three times independently with different amount of ovaries to ensure that the reaction was in the linear range.

X-gal staining

Ovaries of the transgenic lines were dissected, fixed in 2% glutaraldehyde in PBS for 30 min, washed two times in PBS, and stained with 0.25% 5-bromo-4-chloro-3-indolyl β-D-galactopyranoside (X-gal) at 37^0C for 2 hr in buffer 0.15 M NaCl, 10 mM NaH_2PO_4 (pH 7.5), 1 mM $MgCl_2$, 3.1 mM $K_3[FeII(CN)_6]$, and 3.1 mM $K_4[FeIII(CN)_6]$.

Combined RNA and DNA FISH

At first, RNA-RNA hybridization with DIG-labeled strand-specific riboprobe was done. The *TART* probe contained a fragment of the ORF2 corresponding to nucleotides 2377-2888 of the GenBank sequence DMU02279. The *HeT-A* probe contained a fragment of the ORF (nucleotides 4330-4690 of the GenBank sequence DMU06920). Hybridization conditions used at this stage allowed us to detect RNA rather than genomic DNA. To exclude the possibility of RNA-DNA hybridization in this stage an RNaseH control was done in the preliminary experiments (27). After RNA hybridization ovaries were incubated with 1% H_2O_2 in PBS for 30 min to inactivate endogenous peroxidase. Then samples were incubated for 1 h with anti-DIG-POD antibodies (Roche) (diluted at 1:1000), washed 3 times in PBS and incubated with fluorescein-conjugated tyramide (0,1 mg/ml) diluted in 0,0015% H_2O_2 at 1:25 for 30 min. Tyramide binds covalently to the tyrosine residues of the adjacent proteins in the presence of

peroxidase activity. This provides protection of RNA FISH signal in the subsequent DNA FISH procedure. Genomic DNA FISH was performed as described (37). After DNA hybridization ovaries were incubated with avidin-rhodamin (Vector Labs) (diluted at 1:500). To stain DNA, samples were incubated in PBS containing 0.5 μg/ml DAPI. The ovaries were finally mounted in SlowFade Gold media (Invitrogen) and then visualized by confocal microscope Zeiss LSM510Meta.

Does NRO assay reflect in vivo transcription status?

Nuclear run-on assay is applied to estimate a transcriptional status of the locus. Addition of nucleotides to the isolated nuclei results in the extension of nascent RNAs that are associated with transcriptionally engaged polymerases under conditions when reinitiation is prohibited. Sarkosyl is often added to the nuclear run-on reaction to prevent new transcription initiation events. However, several considerations suggest that no transcription initiation occurs during nuclei isolation and run-on reaction even in the absence of sarkosyl. Experiments of Cook's lab that utilized a combination of in vivo labeling of nascent transcripts with BrUTP followed by in vitro labeling with biotin-CTP have shown that no new initiation occurs in nuclei since all biotin-CTP sites are also labeled with BrUTP (45). These experiments were carried out in the absence of sarkosyl. In run-on experiments performed in Zamore's lab (46), it was shown that after about 40 minutes, transcriptional rates saturated consistent with RNA pol II having elongated all available transcripts without reinitiating new rounds of transcription. These experiments were also done in the absence of sarkosyl with *Drosophila* ovarian tissues. According to the dynamic curve represented in this work (46), the amount of run-on RNA is increased up to 30 min, thus, to obtain the amount of run-on RNA sufficient for subsequent RT-PCR, we kept run-on reaction for 30 minutes in the absence of sarkosyl. The problem is that ovarian cells have the genome of a high ploidy index (up to 1024 haploid DNA value). Sarkosyl, in the final concentration of 0.2-1%, which is used in different run-on protocols, results in nuclei lysis and appearance of a high viscosity of the solution. This may impede buffer component diffusion. Decrease of the starting amount of material results in a low amount of the run-on RNA fraction. Thus we carried out NRO assay for 30 minutes in the absence of sarkosyl. We performed additional controls to confirm reliability of the results obtained under the conditions chosen in our experiments. NRO analysis was done for w^{1118} and *si_piwi* ovaries during 5 or 30 minutes in the presence or absence of sarkosyl (Supplementary Fig.1). We have shown that duration of reaction and the presence/absence of sarkosyl do not affect the main result, namely, accumulation of the retrotransposon run-on transcripts in the *piwi* knockdown ovaries. An increase in run-on RNA amount was observed in the presence of sarkosyl. Actually, sarkosyl removes chromatin proteins therefore engaged polymerases elongate on naked DNA faster than on histone-covered DNA. Most likely, the event of transcription reinitiation in isolated and washed nuclei is very unlikely even in the absence of sarkosyl owing to the high energy requirements of promoter DNA unwinding.

Other processes such as co-transcriptional RNA degradation or processing do not occur in the run-on reaction as well. We have shown enrichment of NRO RNA fraction by non-processed transcripts since splicing is not effective after nuclei isolation. Abundance of spliced and unspliced *rp49* transcripts are similar in the NRO RNA fraction, while in the total nuclear RNA, the amount of unspliced *rp49* transcripts is ~50 times less than that of processed ones (not shown). Actually, enrichment of NRO libraries by intronic sequences and highly unstable transcripts (44) indicates that processing and RNA degradation in isolated nuclei are inhibited. In the experiments of Zamore's lab (46), dynamic curves of the run-on labeling for housekeeping genes (*rp49* and *actin*) and retrotransposons (*HeT-A, roo, I*-element and *gypsy*) are similar, which indicates no piRNA-mediated co-transcriptional degradation of the retrotransoson transcripts (if any) in the isolated ovarian nuclei. This experiment was performed without sarkosyl during 60 minutes. We made dynamic curves (0-60 minutes) of *rp49* and *HeT-A*

accumulation for w^{1118} and *si_piwi* ovaries (Supplementary Fig. 2). First, these curves demonstrate similar rates of *rp49* and *HeT-A* run-on transcripts accumulation in the w^{1118} and *si_piwi* ovaries. This fact indicates that no piRNA-mediated post-transcriptional degradation of *HeT-A* transcripts occurs in isolated nuclei of the control line. Second, this experiment shows that transcriptional rate saturates after 30 minutes, thus, no transcription reinitiation events occur under these conditions. At last, the amount of run-on RNA is increased up to 30 minutes. Thus, we performed NRO assay under appropriate conditions which allowed us to estimate transcriptional rate at the locus of interest.

Estimation of enrichment and purity of NRO RNA fraction

Enrichment and purity of immuno-purified BrUTP-labeled RNA were estimated in preliminary experiments using in vitro synthesized RNAs. Firefly and Renilla luciferase genes (lucF and lucR, respectively) cloned in pBS SK^- were used for in vitro transcription. BrUTP-labeled lucR RNA mixed with "cold" lucF RNA (in the ratio 1:1) were immuno-precipitated according to described scheme (Supplementary Fig.3). Then we estimated the ratio of both RNAs in purified fraction by RT-qPCR. Amount of "cold" lucF RNA was ~2000 times less than BrUTP-lucR RNA. Later, addition of "cold" lucF and BrUTP-labeled lucR RNAs to run-on RNA samples before immuno-purification and subsequent RT-qPCR of purified RNA were used for a control of purification in each experiment.

Next, we estimated, if the contamination by "cold" nuclear RNA could influence the analysis of NRO RNA. We performed a NRO reaction with the ovaries of homozygous *spn-E* mutants in the presence of BrUTP or UTP. After immunoprecipitation reverse transcription was carried out on the purified fraction for each RNA samples. Amount of *rp49* and *HeT-A* transcripts was compared by RT-qPCR in both samples. In BrUTP NRO RNA, both transcripts were 50-fold more abundant than in UTP NRO RNA. Thus, contaminant RNA represents ~2% of the final NRO RNA, corresponding to 98% purity for BrUTP-RNA. This result shows that NRO RNA is highly enriched for BrUTP-RNAs relative to contaminant RNAs providing desired specificity of this method.

Northern analysis

RNA samples (20 μg per lane) were separated on formaldehyde/agarose gels and transferred to Hybond-XL membrane (Amersham). RNA Millennium marker (Ambion) was used. P^{32}-labeled riboprobes corresponding to antisense strands of *TART* and *HeT-A* were synthesized. PCR fragments of retrotransposons cloned into pBS SK^- were used as transcription templates. The *TART* probe contained a fragment of the ORF2 corresponding to nucleotides 2377-2888 of the GenBank sequence DMU02279. The *HeT-A* probe contained a fragment of the ORF (nucleotides 4330-4690 of the GenBank sequence DMU06920). As a loading control, hybridization with an *rp49* probe was used. Hybridization was performed at 60°C overnight in 0.5 M NaCl, 0.1 M sodium phosphate (pH 7.5), 25 mM EDTA, 1% SDS, 50 μg/ml denatured salmon sperm DNA, 5x Denhardt's solution, 50% formamide. The filters were washed three times at 60°C with solution containing 10 mM sodium phosphate and 0.2% SDS and visualized by phosphor imager Storm-840 (Amersham).

Supplementary Figures

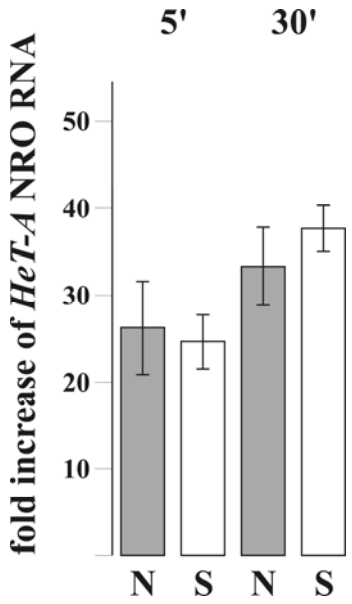

Supplementary Fig. 1 **Nuclear run-on analysis of *HeT-A* transcription in the absence and presence of sarkosyl.** Bars of histograms represent a ratio of *HeT-A* to *rp49* transcript abundance in the *si_piwi* flies related to this ratio in w^{1118}. ***N*** represents the run-on protocol we used in this study. ***S*** indicates the addition of 0.4% sarkosyl**.** Duration of the run-on reaction is indicated.

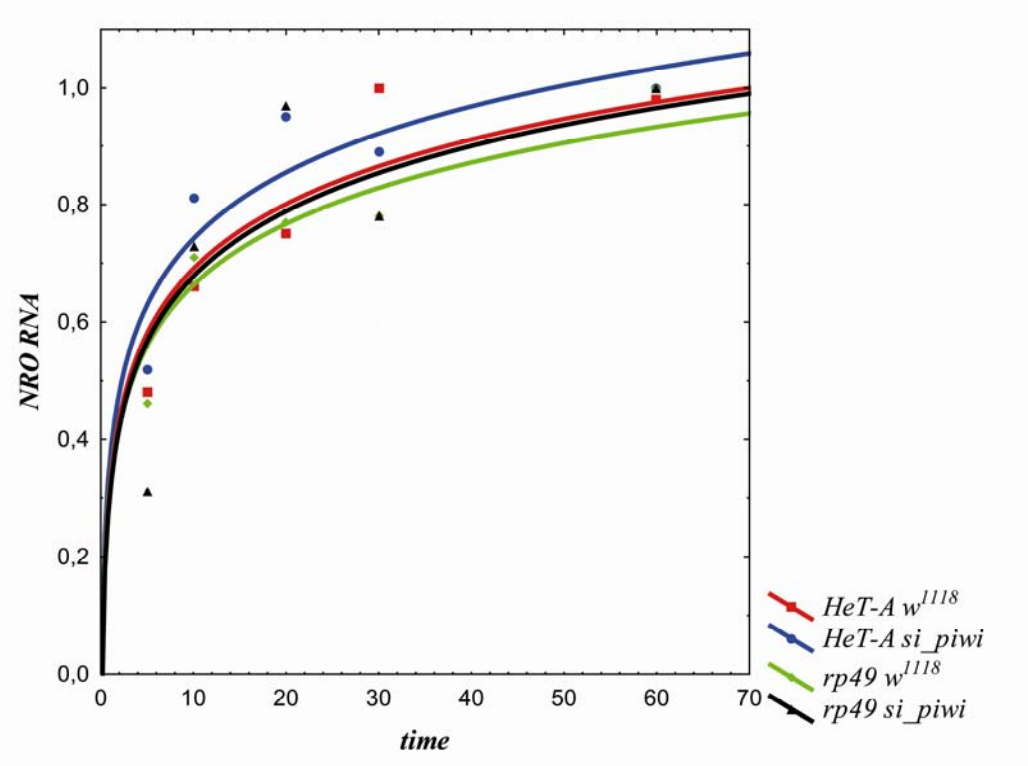

Supplementary Fig. 2 **Dynamic curves of the NRO transcripts accumulation.** *rp49* and *HeT-A* transcript amounts were estimated by qRT-PCR of the run-on RNA fraction from w^{1118} and *si_piwi* ovaries. Normalization to the BrUTP-labeled lucR RNA, which was added to the run-on buffer prior the reaction, was done. Duration of reaction is indicated in minutes.

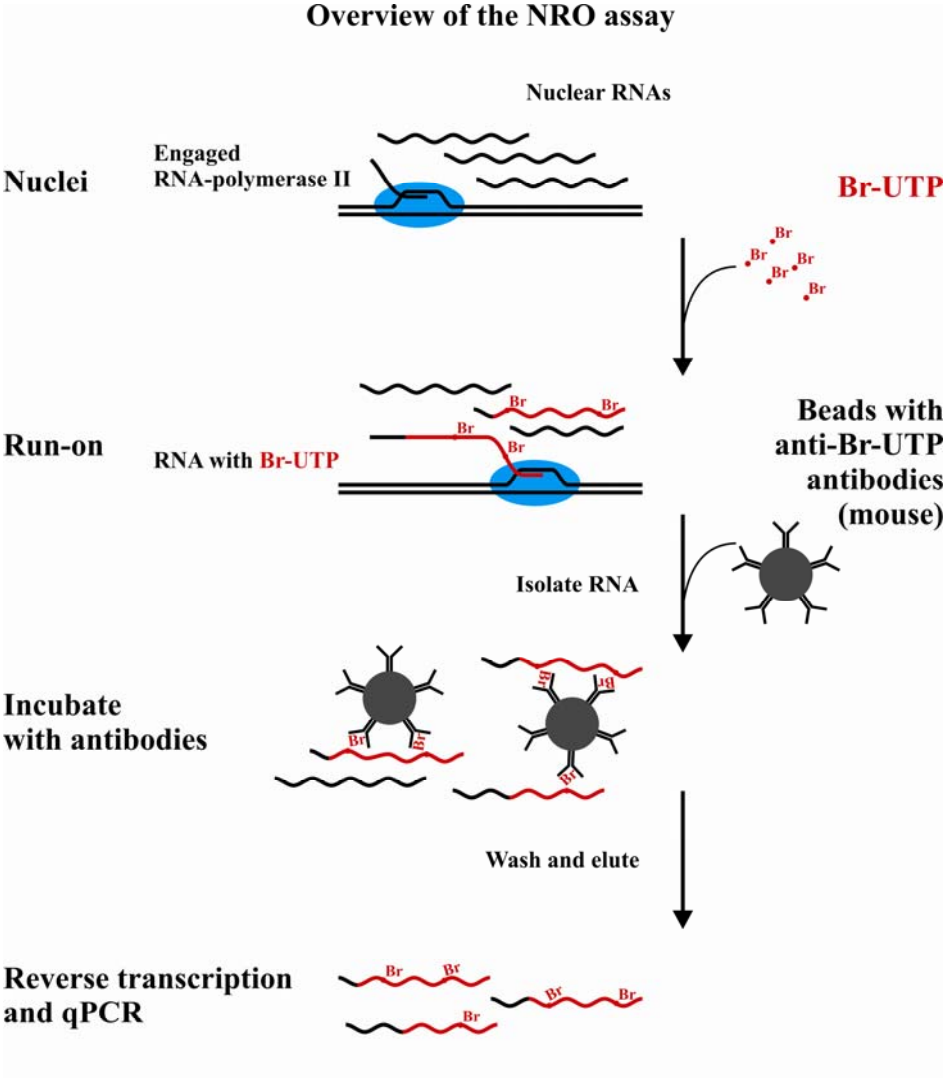

Supplementary Fig. 3 **Overview of the NRO assay.** A schematic representation of the steps of the run-on transcription using Br-UTP and immuno-purification of the Br-UTP-labeled RNA fraction.

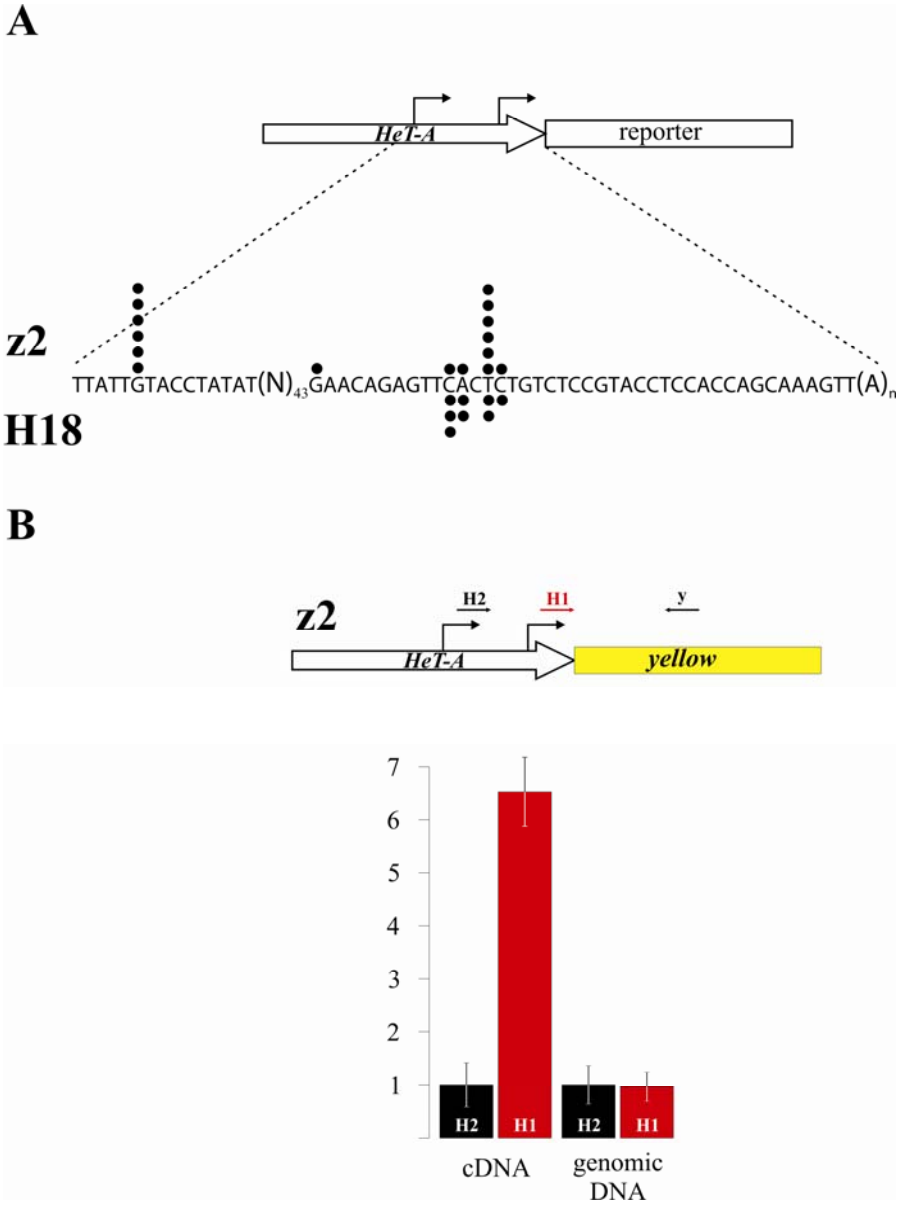

Supplementary Fig.4 **Positions of the transcription initiation sites in the *HeT-A/yellow* (z2 line) and *HeT-A/lacZ* (H18 line) constructs identified by 5' RACE. A** A schematic representation of the *HeT-A*-containing constructs is given. Positions of the transcription start sites are indicated by arrows. The sequence is a fragment of the *HeT-A* element z2 represented in both reporter constructs. The dot designates a single detected transcription initiation sites at the specific nucleotide, determined for the *HeT-A/yellow* construct (above sequence) and for the *HeT-A/lacZ* construct (under sequence) using 5' RACE analysis of ovarian RNA from the z2 and H18 lines, respectively. **B** Main transcription start site is located -30 bp upstream of the *HeT-A* polyadenylation site. Schematic representation of the *HeT-A/yellow* construct and the primers are shown. Histograms on the right represent qPCR on the genomic DNA of the z2 line with H1-y and H2-y primers normalized to the *rp49* demonstrating similar working efficiency of the primers. Histograms on the left show result of the RT-qPCR analysis with the same pair of primers demonstrating that most of the transcripts are generated from -30 transcription start site. The bars of histograms represent a ratio of *HeT-A/yellow* to *rp49* transcript abundance in the ovaries of *z2* flies.

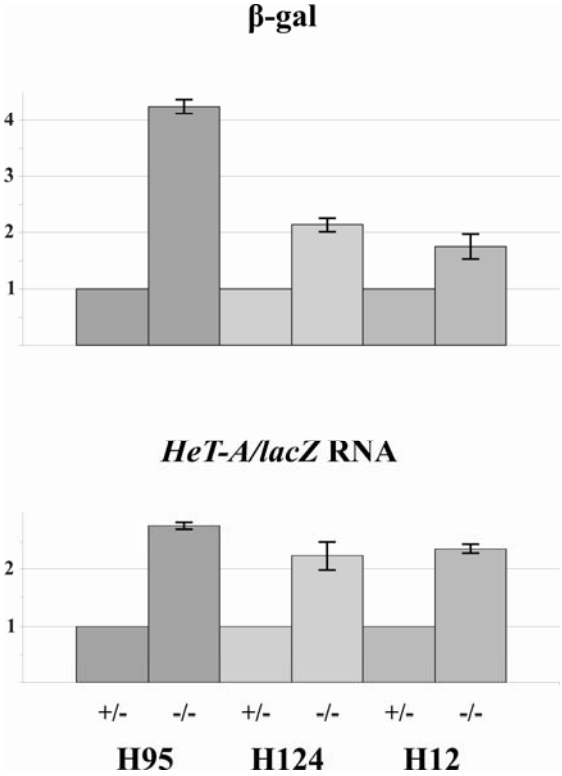

Supplementary Fig.5 **Derepression of the *HeT-A/lacZ* transgene expression in the ovaries of *spn-E* mutants.** H12, H95 and H124 are the transgenic lines with euchromatic transgene localization bearing *spn-E* mutations. Upper panel represents quantitative measurement of the β-galactosidase activity in the ovaries of *spn-E*^{1}/+ (+/-) and *spnE*^{1}/*spn-E*^{hls3987}(-/-) flies normalized to the total protein amount in the lysate estimated by Bradford method. β-galactosidase activity in the +/- flies is designated as 1. Lower panel shows RT-qPCR analysis of the RNA isolated from the ovaries of *spn-E*^{1}/+ and *spnE*^{1}/*spn-E*^{hls3987} transgenic flies. The bars of histograms represent a ratio of *HeT-A/lacZ* to *rp49* transcript abundance in the ovaries of *spn-E*^{1}/*spn-E*^{hls3987} flies related to this ratio in *spn-E*^{1}/+ females. Quantitative estimation of transgene silencing in *piwi* mutants was not performed, since the *piwi*^{2}/*piwi*^{3} ovaries are extremely degenerated.

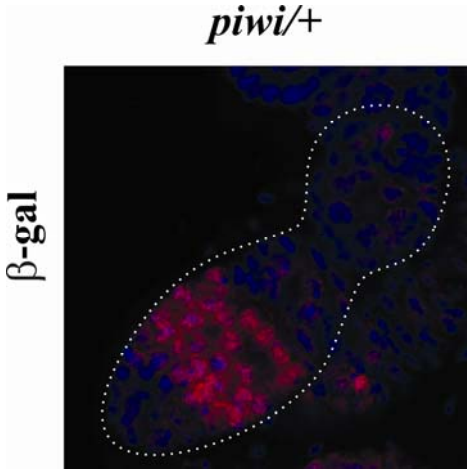

Supplementary Fig.6 ***HeT-A-lacZ*** **expresses in the germarium of the *piwi/+* ovaries**. Immunostaining of β-galactosidase using rabbit polyclonal antibodies ab4761 (Abcam, diluted at 1/500). β-galactosidase (red) is revealed in the germarium cysts. DNA was stained with DAPI (blue). Dashed line indicates the boundary of germarium.

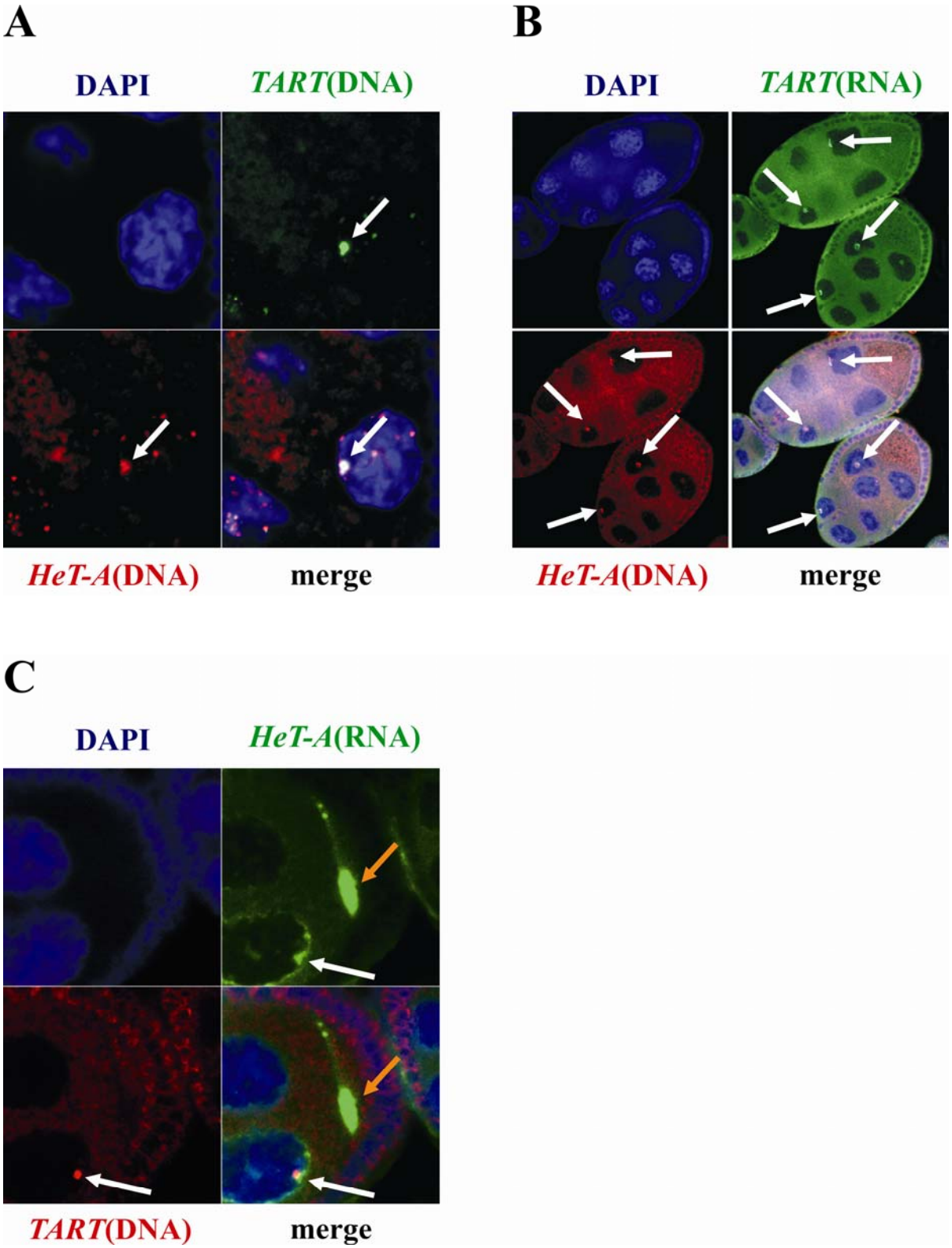

Supplementary Fig.7 **Telomeric retroelement transcripts accumulate in telomeric regions of the nurse cell nuclei in *spn-E* mutants. A** DNA FISH analysis demonstrates colocalization of *TART* (green) and *HeT-A* (red) probes which indicates that these probes stain telomeres of the nurse cell chromosomes. **B** Antisense *TART* transcripts (green) are colocolized with the *HeT-A* DNA probe (red) which serves here as a marker of telomere. **C** Sense *HeT-A* transcripts (green) are colocolized with the *TART* DNA probe (red) in nucleus. Orange arrow indicates *HeT-A* transcript accumulation in the cytoplasm of oocyte. The results were obtained by combined RNA and DNA FISH with strand-specific riboprobe and DNA probe, respectively. Ovaries were dissected from *spn-E*^{1}*/spn-E*^{hls3987} flies. DNA was stained with DAPI (blue).

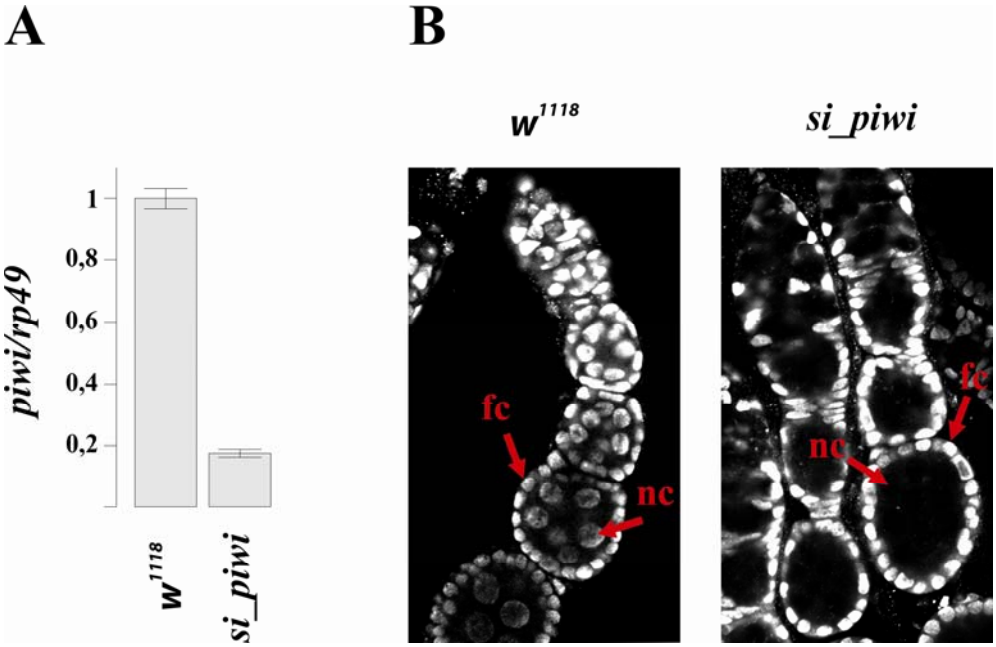

Supplementary Fig.8 **PIWI expression in the RNAi *piwi* flies.** In *si_piwi* flies, GAL4 drives expression of the *piwi* hairpin in ovarian germ cells (Supplementary Materials and Methods). **A** RT-qPCR analysis of the *piwi* expression demonstrates a decrease in the *piwi* transcripts abundance in the ovaries of *si_piwi* flies. The bars of histograms represent a ratio of *piwi* to *rp49* transcript abundance in the ovaries. **B** Immunostaining using rabbit anti-PIWI antibodies (kindly provided by G. Hannon) reveals no PIWI protein in the germinal cells of the *si_piwi* flies. fc – follicular cells, nc – nurse cells.

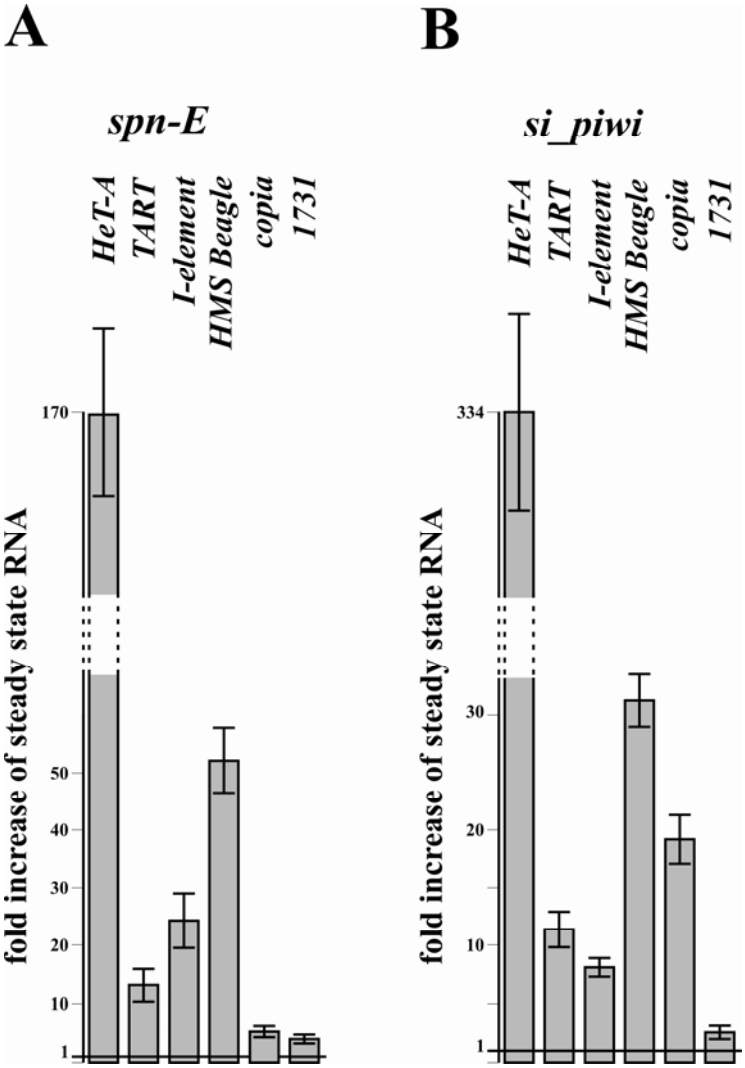

Supplementary Fig.9 **Accumulation of retrotransposon transcripts in the *spn-E/spn-E* and *si_piwi* ovaries.** RT-PCR analysis was done to compare retrotransposon transcript amounts in the total ovarian RNA from *spn-E* (**A**) or *si_piwi* ovaries (**B**). The bars of histograms represent a ratio of retrotransposon to *rp49* transcript abundance in the ovaries of transheterozygous *spn-E*^{1}*/spn-E*^{hls3987} flies related to this ratio in *spn-E*^{1}*/TM3* heterozygous females (A) or in *si_piwi* related to *w*^{1118} ovaries (B).

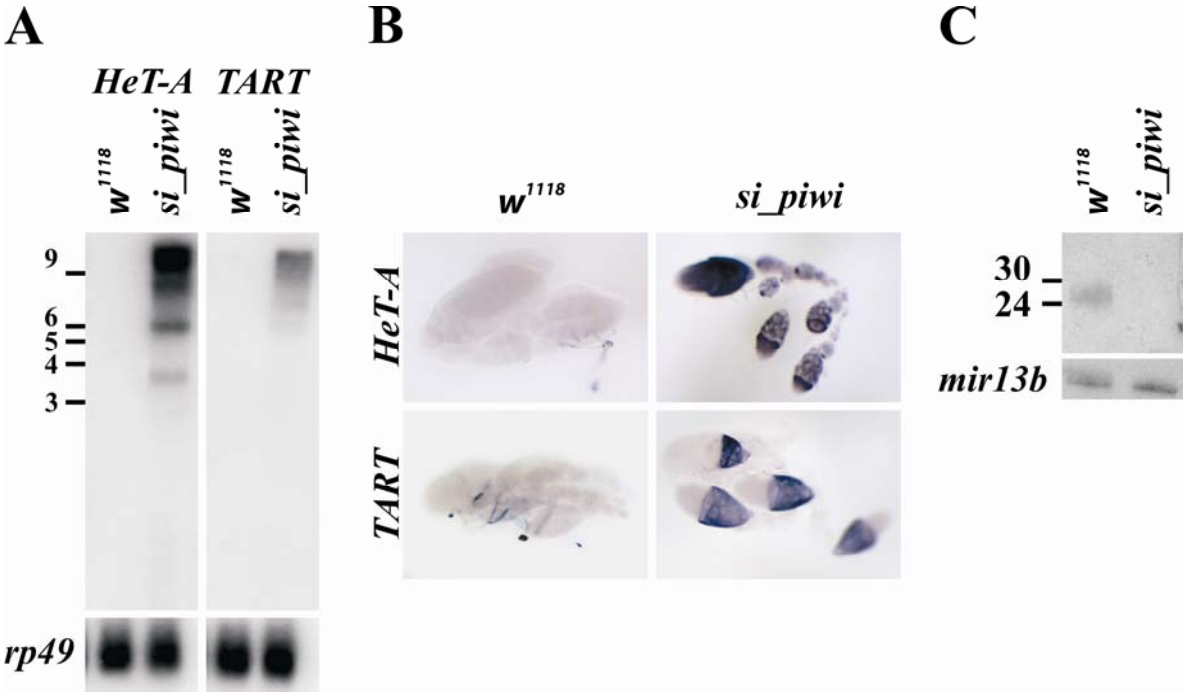

Supplementary Fig.10 **Derepression of the telomeric retrotransposons in the ovaries of *si_piwi* flies. A** Northern analysis of sense *HeT-A* and *TART* transcripts. Total ovarian RNAs from *si_piwi* and control flies were analyzed. Hybridization with *HeT-A* and *TART* antisense riboprobes was performed. The lower panels demonstrate hybridization with the *rp49* probe as a loading control. Sizes of RNA Millennium Markers (Ambion) are indicated in kb. Strong accumulation of sense *HeT-A* and *TART* transcripts is observed in the ovaries of *si_piwi* flies. **B** *in situ* RNA hybridization with *HeT-A* (upper panels) and *TART* (lower panels) antisense riboprobes, using anti-DIG AP-conjugated antibodies. Ovaries were dissected from *si_piwi* and control flies. *HeT-A* transcripts accumulate at all stages of oogenesis in the oocyte and nurse cells while *TART* transcripts are detected at later stages of oogenesis. **C** Northern analysis of *HeT-A* piRNAs in the ovaries of *si_piwi* flies. RNA was isolated from the ovaries of *si_piwi* and w^{1118} flies using the miRACLE miRNA isolation kit (Stratagene). Hybridization with sense *HeT-A* riboprobe corresponding to the 3' UTR reveals short RNAs of 27-29 nt in size in control flies but no signal in ovaries of *si_piwi* flies. Lower panel represents hybridization with oligonucleotide complementary to the *mir-13b1* microRNA. P^{33}-labeled RNA oligonucleotides were used as size markers.

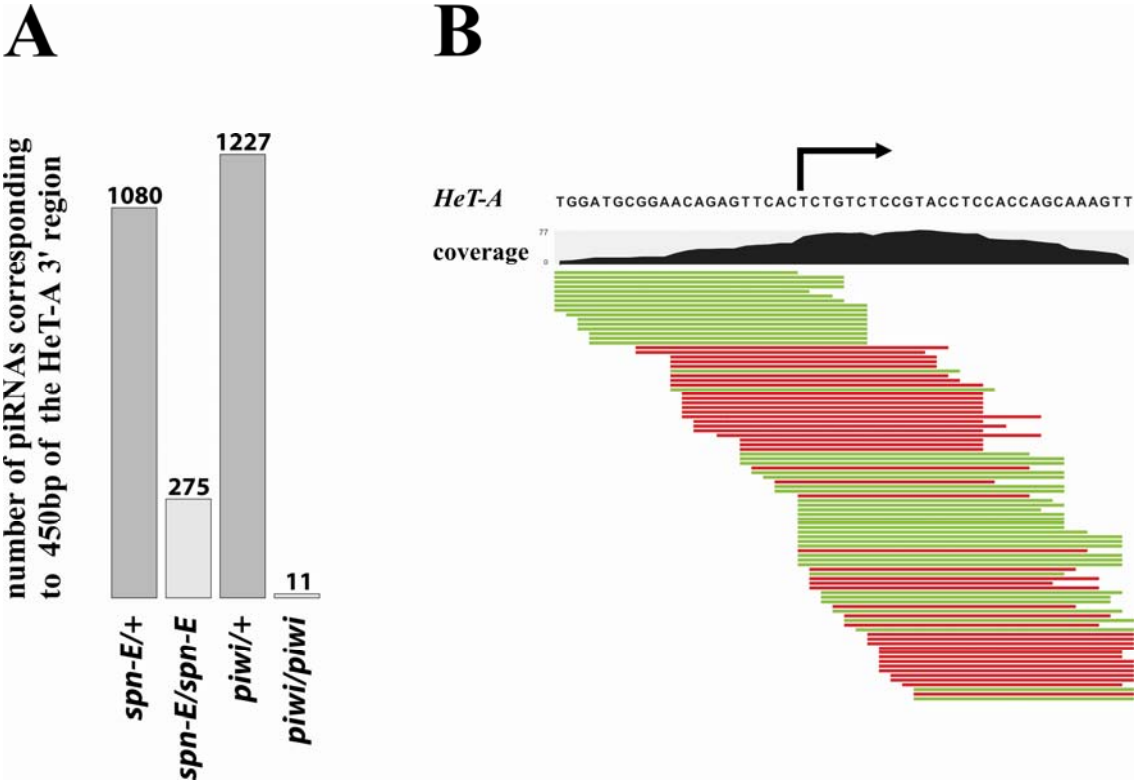

Supplementary Fig.11. ***HeT-A*-specific piRNAs in the piRNA pathway mutants** (datasets of short RNA libraries from (47)) **A** Amount of piRNAs complementary to the 3' *HeT-A* fragment cloned in the *HeT-A/lacZ* construct in *spn-E* and *piwi* mutants compared to their respective heterozygotes. **B** Densities of ovarian sense (red) and antisense (green) piRNAs over the *HeT-A* 3' fragment in *spn-E/+* are shown. -30 *HeT-A* transcription start site is indicated.